SUPPORTING INFORMATION:

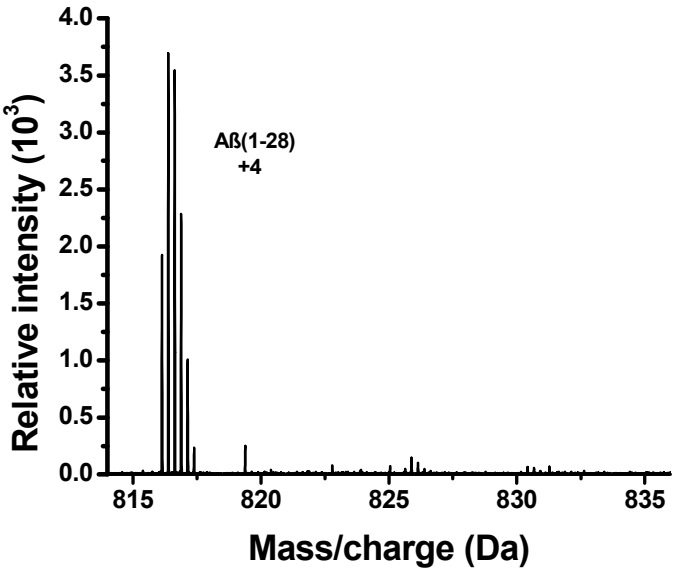

Figure S1. A portion of a positive-ion ESI-FTICR mass spectrum of Aβ (1-28) showing the quadruply charged ion of Aβ(1-28).

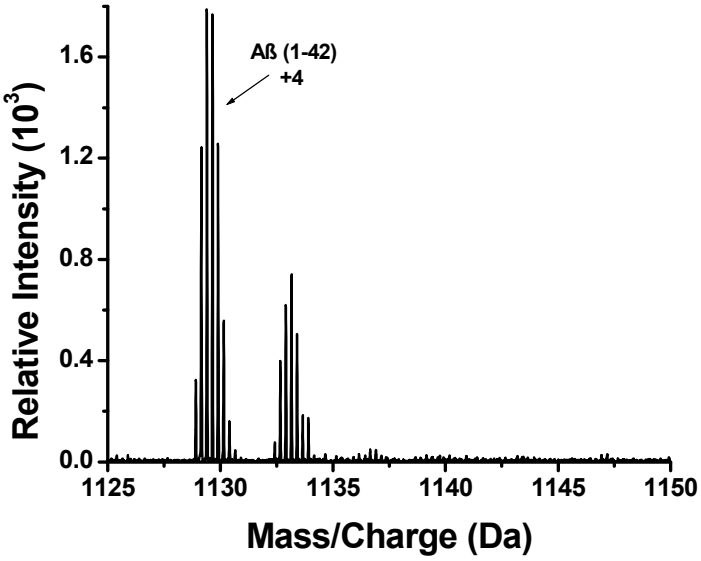

Figure S2. A portion of a positive-ion ESI-FTICR mass spectrum showing the quadruply charged ion of Aβ (1-42).

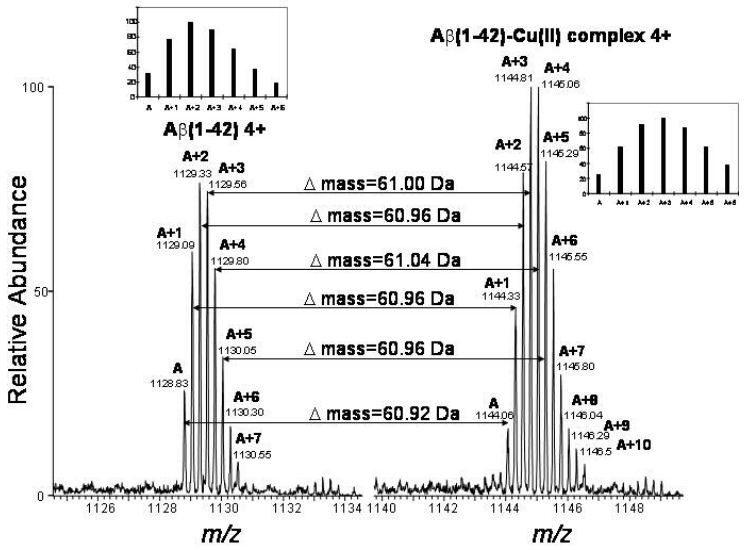

Figure S3. High-resolution mass spectrum of quadruply charged Aβ(1-42) and Aβ(1-42)-Cu(II) complex ions acquired on an linear-ion trap mass spectrometer operated in the high resolution, "ultra zoom scan" mode. A solution with an Aβ(1-42)/Cu(II) molar ratio of 1:10 was employed for the measurement. Inset: theoretical isotopic distribution profiles of quadruply charged ions of Aβ(1-42) and Aβ(1-42)-Cu(II) complex.

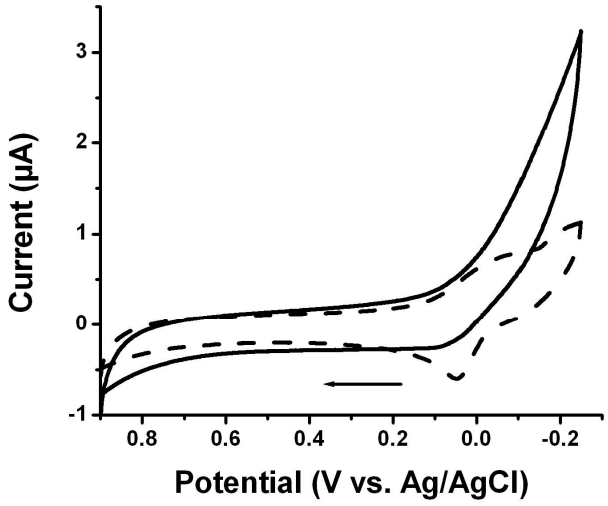

Figure S4. CVs of 100 μM Cu(II) in an air-saturated 10 mM phosphate buffer solution (pH 7.4) containing 0.1 M Na_2SO_4 (solid curve) and a N_2-purged solution (dashed curve). A glassy carbon electrode with a diameter of 3 mm was used. The scan rate was 0.020 V/s. The arrow indicates the initial scan direction.

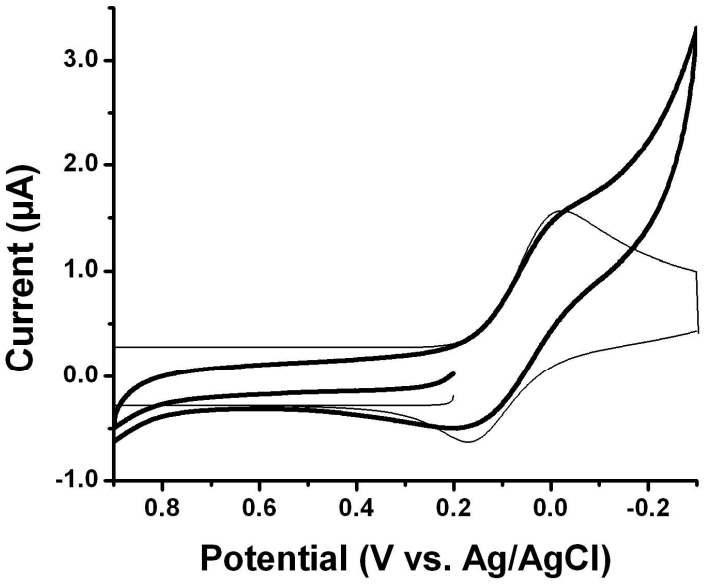

Figure S5. Simulated (thin solid curve) and experimental (thick solid curve) CVs of Aβ(1-16)-Cu(II) in the presence of O_2. The rate constant used for the one-electron reduction of Aβ(1-16)-Cu(II) complex was 5×10^{-4} s^{-1} and the redox reaction rate constant for the follow-up O_2 reduction to H_2O_2 and regeneration of Aβ(1-16)-Cu(II) was 1×10^3 $M^{-1}s^{-1}$.

Simulation of the electron transfer process in Figure 3 was conducted with a CH simulation program. In performing the simulation, diffusion coefficients of 3×10^{-6} cm^2s^{-1} were used for the Aβ(1-16)-Cu(II) and Aβ(1-16)-Cu(I) complexes, based on the measured diffusion coefficient of a similar Aβ peptide.(*cf. Reference 1*) A diffusion coefficient of 1×10^{-6} cm^2/s was used for O_2. The concentration of Aβ(1-16)-Cu(II) was estimated to be *ca.* 0.2 mM by using the complexation constant of 1×10^7 M^{-1} (*cf. Reference 2*). The electrode surface area is 0.071 cm^2, and the double-layer capacitance of the electrode is 14 μF. The O_2 concentration used is 0.26 mM, which is a value commonly found in an air-saturated aqueous solution.

In carrying out the simulation, we ignored the electrolytic reduction of O_2 at the electrode and the possible electroreduction of any uncomplexed Cu^{2+} in the solution. Both of these reductions occur right after the Aβ-Cu(II) reduction and might have contributed to the rising portion of the reduction current beyond 0.0 V. Despite these complications, the simulated and experimental voltammograms are in reasonable agreement, confirming the proposed mechanism (equations 1-2 in the text).

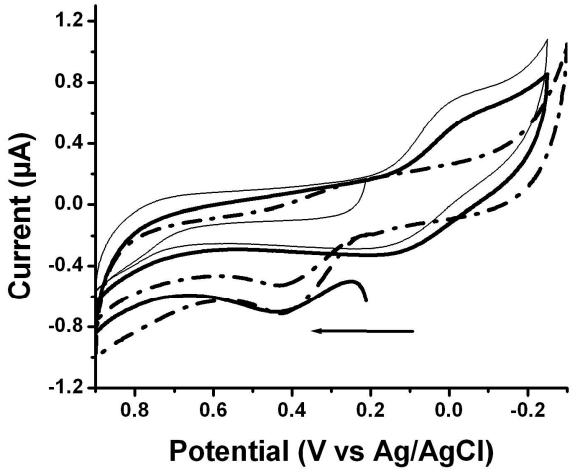

Figure S6. CVs of 100 μM ascorbic acid (dash-dot-dash curve), a mixture of 200 μM Aβ(1-16), 200 μM Cu(II), and 200 μM ascorbic acid (thin solid curve), and a solution containing 200 μM Aβ(1-16), 200 μM Cu(II), and 400 μM ascorbic acid (thick solid curve) in 10 mM phosphate buffer containing 0.1 M Na_2SO_4 (pH 7.4). A glassy carbon electrode with a diameter of 3 mm was used. The scan rate was 0.020 V/s. The arrow indicates the initial scan direction.

In acquiring the CVs, the potential was scanned from 0.2 V to 0.9 V to initiate the possible oxidation of ascorbic acid and continued to the cathodic direction to observe the reduction of Aβ(1-16)-Cu(II) complex. Notice that the ascorbic acid oxidation peak disappeared during the second potential scan in the thick solid curve, whereas the ascorbic acid oxidation peak was well-defined and substantial when the Aβ(1-16)-Cu(II) complex was absent (see the second potential scan in the dash-dot-dash curve).

Table S1: Extracting the copper oxidation state from mass spectral peaks of the Aβ(1-42)-Cu(II) complex. A solution with an Aβ(1-42)/Cu(II) molar ratio of 1:10 was used for ESI-MS measurement**.**

Aβ(1-42): Cu^{2+} 1:10				Aβ(1-42)-Cu(II)			Aβ(1-42)-Cu(I)		
		Meas. *m/z*	Meas. Rel. Abund. (%)	Calcd. *m/z*	Calcd. Rel. Abund. (%)	Dev. (ppm)	Calcd. *m/z*	Calcd. Rel. Abund. (%)	Dev. (ppm)
4+ Ion	A	1144.06	16	1144.05	25	6	1144.31	25	215
	A+1	1144.30	49	1144.30	62	4	1144.56	62	198
	A+2	1144.55	86	1144.55	92	4	1144.81	92	207
	A+3	1144.80	100	1144.81	100	5	1145.06	100	216
	A+4	1145.04	99	1145.06	87	14	1145.31	87	216
	A+5	1145.29	79	1145.31	62	14	1145.56	62	234
	A+6	1145.53	50	1145.56	37	23	1145.81	37	226
	A+7	1145.78	27	1145.81	20	24	1146.06	20	226
	A+8	1146.04	18	1146.06	9	15	1146.31	9	235
	A+9	1146.29	10	1146.31	4	16	1146.56	4	235

Table S2. The reduction peak currents recorded at different Aβ/Cu(II) molar ratios. The Aβ concentration was kept at 200 μM while varying the Cu(II) concentration. All the solutions were air-saturated.

Aβ(1-16)/Cu(II) molar ratio	I_{pc} (μA)
4:1	0.31
2:1	0.65
4:3	0.92
1:1	1.25

References used to select some of the parameters for the simulation:

(1) Mansfield, S. L., Jayawickrama, D. A., Timmons, J. S., and Larive, C. K. (1998) Measurement of peptide aggregation with pusled-field gradient nuclear magnetic resonance spectroscopy. *Biochim. Biophys. Acta 1382*, 257-265.

(2) Syme, C. D., Nadal, R. C., Rigby, S. E. J., and Viles, J. H. (2004) Copper binding to the amyloid-beta peptide associated with Alzheimer's disease. *J. Biol. Chem. 279*, 18169–18177.